ISSN 0029-3865

BR99B1094

CBPF - CENTRO BRASILEIRO DE PESQUISAS FÍSICAS
Rio de Janeiro

Notas de Física

CBPF-NF-044/98
June 1998

Effective liquid drop description for alpha decay of atomic nuclei

O A P Tavares, S B Duarte, O Rodriguez, F Guzmán, M Gonçalves and F García

30 - 10

CNPq - Conselho Nacional de Desenvolvimento Científico e Tecnológico

CBPF-NF-044/98

Effective liquid drop description for alpha decay of atomic nuclei

*O A P Tavares, S B Duarte, O Rodríguez**, *and F Guzmán**

Centro Brasileiro de Pesquisas Físicas — CBPF/CNPq,
Rua Dr. Xavier Sigaud 150, 22290-180 Rio de Janeiro-RJ, Brazil

M Gonçalves†

Instituto de Radioproteção e Dosimetria — IRD/CNEN,
Av. Salvador Allende s/n, 22780-160 Rio de Janeiro-RJ, Brazil

F García*

Instituto de Física, Universidade de São Paulo,
Caixa Postal 66318, 05315-970 São Paulo-SP, Brazil

Alpha decay half-lives are presented in the framework of an effective liquid drop model for different combination of mass transfer descriptions and inertia coefficients. Calculated half-life-values for ground-state to ground-state favoured alpha transitions are compared with available, updated experimental data. Results have shown that the present model is very suitable to treat the alpha decay process on equal foot as cluster radioactivity and cold fission processes. Better agreement with the data is found when the sub-set of even-even alpha emitters are considered in the calculation.

---

*Permanent address: Instituto Superior de Ciências y Tecnologia Nucleares, Av. Salvador Allende y Luaces, Apartado Postal 6163, La Habana, Cuba.

†Author to whom correspondence should be sent: telo@ird.gov.br.

I. INTRODUCTION

The alpha-decay process was interpreted in the early 20's in terms of tunnelling through a quantum mechanical potential barrier [1]. In recent years, two theoretical extreme approaches have been developed: the cluster- and fission-like theories [2]. While in cluster-like approaches the alpha emission is treated in a natural way, in fission-like theories the alpha-decay process is considered as a very asymmetric fragmentation of the parent nucleus. The main difference between these two descriptions consists in the behavior of the system before the formation of the nascent fragments, and the correspondent potential energy surface. However, in both approaches the potential barriers are identical outside of the touching configuration of the separating fragments.

A large number of new experimental and theoretical investigations on alpha-decay half-life has been developed during the last three years or so [3–15]. On one hand the studies have been mainly motivated by the interest in searching for the heaviest elements, since their alpha-decay chains provide signatures of the structure of the nuclei which start the decay sequence. Recently, the heaviest α-decaying nuclei ${}^{269}110$ [16], ${}^{273}110$ [3], ${}^{272}111$ [17], and ${}^{277}112$ [18] have been discovered. The main decay mode for such nuclides with neutron number in the range 159–165 is expected to be the alpha emission mode rather than the spontaneous fission process. The experimental evidences follow the studies on the emission properties of the element $Z > 100$, and points out to the existence of a strong shell closure at $N = 162$ [3].

On the other hand, experimental efforts have been focused on the improvement of the measurements on alpha energies and half-lives from exotic nuclei. In particular, the alpha-decay process offers peculiar information concerning the spectroscopy of extremely neutron deficient nuclei in the region $N > 82 > Z$ [4], taking into consideration that a detailed structure information on energy levels can be determined from decays from ground and isomeric states. Specifically, when analyzing the alpha-decay characteristics of neutron-deficient ${}^{190}Po$, ${}^{189}Bi$ and ${}^{186}Pb$ isotopes, Andreyev *et al.* [5] reported improved values on alpha energies and half-lives, thus giving clear characterization of the behavior of such exotic systems.

At the same time, alpha-decay studies of neutron-deficient isotopes provide information on the nuclear mass surface close to the proton drip line. Due to the small production rates in the heavy element region ($Z > 82$), a detailed spectroscopy information is rarely available. Leino *et al.* [6] have identified two alpha-decay states of the new isotope ^{203}Ra with a sophisticated technique for studying the alpha-decay characteristics. However, it was not possible to draw a definitive conclusion about the effect of deformation on alpha-decay energies in this region of isotopes. This fact is one of the indications calling for substantial improvement in the predictive power of theoretical calculations.

Another topic of interest is that alpha decay favours the population of states in the daughter nucleus with similar spin and parity as the parent nucleus. This property allows to extend the nuclear structure information to several alpha emitters.

Besides the comprehensive work by Buck et *al.* [19–21], and a number of systematic studies on alpha-decay half-life [22–29], new measurements and improved models on alpha decay have been reported recently [30–34].

The aim of the present work is to extend the effective liquid drop model [35–37] to the entire range of available half-life data for the alpha-decay process. Similarly to what has been done in the case for cold fission calculations reported recently [38,39], comparison between the data and the present calculated half-life-values has been performed for different inertia coefficients (Werner-Wheeler's approximation, $\mu_{\rm WW}$, and effective inertia, $\mu_{\rm eff}$), also discussing the use of two mass-transfer constraints (Varying Mass Asymmetry Shape, VMAS, and Constant Mass Asymmetry Shape, CMAS).

In Section 2 the bases of the model concerning shape parameterization, constraint relationships, and the coordinates chosen to describe the configuration of the dinuclear regime are summarized. The alpha-decay half-life calculations are presented in Section 3. The last Section is devoted to conclusion and final remarks.

II. EFFECTIVE LIQUID DROP DESCRIPTION FOR THE ALPHA-DECAY PROCESS

The geometric shape parameterization during the deformation phase of the decaying nuclear system is the same adopted in our previous works [35–38]. The dinuclear phase is parameterized as two intersecting spheres, and two different descriptions are considered for the mass transfer through the window connecting the two fragments, namely, the VMAS and the CMAS descriptions as referred above. In both descriptions the configuration of the nascent fragments is determined by the specification of four independent collective coordinates: the radii of the fragments, R_1 and R_2, the distance between their geometric centers, ζ, and the distance from the center of heavier fragment to the intersecting plane of the spherical fragments, ξ (see Fig. 1 in Ref. [35]).

Theoretical approaches to treat the alpha-decay process have been based on the calculation of the barrier penetrability [1], which is well-defined only for the one-dimensional problem. Thus, three of these collective coordinates should be eliminated preserving the geometric shape and the incompressibility of the nuclear matter. Following the last condition we have imposed that the total volume of the dinuclear system is constant, i.e.,

$$2(R_1^3 + R_2^3) + 3\left[R_1^2(\zeta - \xi) + R_2^2\xi\right] - \left[(\zeta - \xi)^3 + \xi^3\right] - 4R_0^3 = 0 \ , \tag{1}$$

where R_0 is the radius of the parent nucleus.

In order to keep the circular sharp neck connecting the nascent fragments, the following geometric relationship has been introduced

$$R_1^2 - R_2^2 - (\zeta - \xi)^2 + \xi^2 = 0 \ . \tag{2}$$

Finally, an additional constraint relationship distinguishes the two different descriptions of mass transfer (VMAS or CMAS). To characterize the VMAS description we have regarded the radius of the lighter fragment as constant, i.e.,

$$R_1 - \bar{R}_1 = 0 \ , \tag{3}$$

where $\bar{R}_1$ is the final radius of the lighter fragment.

In the CMAS description, on the other hand, the volume of each fragment is set constant, and in terms of the lighter fragment the volume conservation is given by

$$2R_1^3 + 3R_1^2(\zeta - \xi) - (\zeta - \xi)^3 - 4\bar{R}_1^3 = 0 \ . \tag{4}$$

Once the system is reduced to the one-dimensional case, the barrier penetrability factor can be calculated in terms of the geometric separation between the centers of the fragments, ζ, by

$$\mathcal{P} = \exp\left\{-\frac{2}{\hbar}\int_{\zeta_0}^{\zeta_C}\sqrt{2\mu\left[V(\zeta) - Q\right]}\,d\zeta\right\} \ , \tag{5}$$

where ζ_0 and ζ_C are, respectively, the inner and outer turning points, and Q stands for the total kinetic energy available for the final fragments, i.e., the Q-value for decay. The total potential energy, $V(\zeta)$, which appears in equation (5), has been determined by using an analytical solution of Poisson's equation for the Coulomb contribution, and an effective surface potential of a liquid drop for the nuclear component [35]. The experimental Q-value is introduced into the calculation to determine the outer turning point, $\zeta_C = Z_1 Z_2 e^2/Q$, and also to define the surface tension of the drop, by establishing that the difference between the initial and final asymptotic configurations reproduces the experimental Q-value. With this assumption the effective surface tension, σ_{eff}, which is also a function of the atomic numbers of the parent (Z_p), emitted (Z_1), and daughter (Z_2) nuclei, reads

$$\sigma_{\text{eff}} = \frac{1}{4\pi\left(R_p^2 - \bar{R}_1^2 - \bar{R}_2^2\right)} \left[Q - \frac{3}{5}e^2\left(\frac{Z_p^2}{R_p} - \frac{Z_1^2}{\bar{R}_1} - \frac{Z_2^2}{\bar{R}_2}\right)\right] .$$

As usual, the decay rate has been calculated by

$$\lambda = \lambda_0 \mathcal{P} \quad , \tag{6}$$

where λ_0 is a parameter which takes into account the frequency of assaults on the barrier and, partially, the alpha pre-formation probability (not explicitly included in the model). The value of this parameter together with the radius parameter, r_0, are determined in order to get the best agreement with experimental data.

To determine Gamow's penetrability factor we need to know the inertia coefficient, μ, appearing in equation (5). Werner-Wheeler's approximation for the velocity field of the nuclear flow has been largely used in the literature to define the inertia tensor [40]. An alternative proposal for calculating the inertia coefficient has been recently applied with the aim of obtaining half-life estimates for a number of alpha-decay, cluster radioactivity, and cold fission processes [35–38]. By means of straightforward calculation regarding the former constraints (equations (1)–(4)), the expression for the "effective" inertia coefficient reads

$$\mu_{eff} = \mu\alpha^2 \quad , \tag{7}$$

where $\mu = m_1 m_2/(m_1 + m_2)$ is the reduced mass of the nascent fragments, and m_i ($i = 1$, 2) represent their atomic masses. The variable α above takes into account the dependence of the inertia coefficient upon the configuration of the dinuclear system, by considering the constraint relationships on the dynamical evolution of the decaying process. For the VMAS description we have,

$$\alpha^{VMAS} = 1 - \frac{2}{\zeta(R_2-\xi)}\left[(\zeta-\xi)(\bar{z}_1+\bar{z}_2)+\bar{z}_1^2-\bar{z}_2{}^2\right] \quad , \tag{8}$$

where the auxiliary variable $\bar{z}_i$ are given by

$$\bar{z}_1 = \frac{\pi}{4}\left[R_1^2-(\zeta-\xi)^2\right]^2/v_1 \tag{9}$$

$$\bar{z}_2 = \frac{\pi}{4}\left[R_2^2-\xi^2\right]/v_2 \ , \tag{10}$$

and

$$v_1 = \frac{\pi}{3}\left[2R_1^3+3R_1^2(\zeta-\xi)-(\zeta-\xi)^3\right] \quad , \tag{11}$$

$$v_2 = \frac{\pi}{3}\left[2R_2^3+3R_2^2\xi-\xi^3\right] \tag{12}$$

are the volumes of each spherical segment.

For the CMAS description, where the volumes of the fragments are constant, we have

$$\begin{aligned}\alpha^{CMAS} = 1 &+ \frac{1}{v_1}\left[R_1^2-(\zeta-\xi)^2\right]\left[R_1R_1'-(\zeta-\xi)(1-\xi')\right] \\ &+ \frac{1}{v_2}\left(R_2^2-\xi^2\right)\left(R_2R_2'-\xi\xi'\right),\end{aligned} \tag{13}$$

with

$$\frac{d\xi}{d\zeta} = \xi' = -\gamma R_2' \ , \tag{14}$$

$$\frac{dR_1}{d\zeta} = R_1' = \frac{1}{R_1}\left[(\zeta-\xi)+(R_2+\gamma\zeta)R_2'\right] \ , \tag{15}$$

$$\frac{dR_2}{d\zeta} = R_2' = -\frac{(\zeta-\xi)(6R_1+4\zeta-4\xi)+R_1(5R_1+3\zeta-3\xi)}{(R_2+\gamma\zeta)(6R_1+4\zeta-4\xi)+\gamma R_1(5R_1+3\zeta-3\xi)} \ , \tag{16}$$

and

$$\gamma = \left(\frac{6R_2+4\xi}{5R_2+3\xi}\right) \ . \tag{17}$$

The difference between these two inertial coefficients has been already shown in Ref. [38]. There we noticed that the effective inertia coefficient in the CMAS description is the most reduced one, in contrast with the largest values obtained with Werner-Wheeler's inertia calculated in the VMAS description.

III. ALPHA-DECAY HALF-LIFE CALCULATIONS

By regarding the VMAS and CMAS mass-transfer descriptions, and Werner-Wheeler's and the effective inertia coefficients, we were able to obtain the favoured alpha-decay half-life for all alpha emitters of ground-state to ground-state transitions. The mass-values used for both parent and daughter nuclei in each case have been taken from the most recent Mass Table by Audi *et al.* [41]. The choice for the well-controlled parameters of the present model, i. e., the nuclear radius constant, r_0, which appears in the nuclear radius definition ($R = r_0 A^{1/3}$), and the λ_0-parameter has been done in such a way that the quantity

$$\sigma = \sqrt{\frac{1}{N}\sum_{i=1}^{N}\left[\log_{10}\left(\frac{\tau_c^i}{\tau_e^i}\right)\right]^2} \tag{18}$$

is a minimum. Here, τ_c and τ_e represent, respectively, the calculated and experimental alpha-decay half-life values, and N is the number of available experimental data. These latter have been updated from the most recent edition produced by the NNDC (BNL, Upton, N.Y., USA) [42], the latest issues of the Nuclear Data Sheets [43], and from a few papers to some particular cases of alpha decay [16–18,44]. Accordingly, figure 1 shows, as an example, the variation of σ with λ_0 and r_0 for the combination μ_{eff}^{VMAS}. At the minimum of σ, the best λ_0- and r_0-values are then used to construct the distributions depicted in figure 2. These show to be similar to normal distributions centered around the mean value

$$\bar{q} = \frac{1}{N}\sum_{i=1}^{N}\log_{10}\left(\frac{\tau_c^i}{\tau_e^i}\right) , \tag{19}$$

which is rather near to zero for all model descriptions. Table 1 lists the σ-, λ_0-, and r_0-values, as well as the mean values, $\bar{q}$, of the distributions showed in figure 2. As one can see, all model combinations are pretty good in reproducing the data. As a matter of fact, the combination μ_{eff}^{VMAS} is able to fit $\sim$ 80% of the cases within a factor of 3. We remark that the values of r_0 thus obtained for each model combination (table 1) are very close to those found in describing the cluster radioactivity and cold fission processes as reported in Refs. [37,38].

Better agreement between the present calculated results and experimental data is observed in the case for even-even alpha emitters (shown in table 2 and figure 3). For these cases it results that about 90% of the data are reproduced by the calculation model (μ_{eff}^{VMAS} description) within a factor of 3.

Another way to compare our theoretical results with the data is through the plots on figures 4 and 5. In these figures we displayed the quantity $\log_{10}(\tau_c/\tau_e)$ as a function of the neutron number of the parent nucleus. As one can see, good agreement between our results and the data is apparent, except for a few cases, mostly located at the 126 neutron shell closure. These discordant points seem to be related to the inability of our effective model in taking into account the detailed microscopic quantum aspects of the potential barrier, as well as the alpha pre-formation probability near closed neutron shell. A similar behaviour is noticed when one deals with the sub-set of even-even alpha-emitters, as illustrated in figure 5. Here, we can clearly see that the predictive power of the model is rather good.

Finally, for the sake of direct comparison between calculated and experimental alpha-decay half-life-values, we present in table 3 such data for 388 alpha emitters.

IV. CONCLUSION AND FINAL REMARKS

In the present work the effective liquid drop model, which has been successful in describing cluster emission and cold fission processes [35–38], has been submitted to a detailed analysis in reproducing the most recent and complete set of existing experiment data for alpha decay half-life. We have concluded that a fairly good agreement is reached without any change in the model, only providing it with the appropriate adjustment of only two model parameters, r_0 and λ_0. We believe that this analysis has given this simple model a significant degree of confidence as a powerful predictable tool also for alpha decay half lives. The quality of the various fits to the data base, using different combinations of inertial coefficients and shape parametrization, results comparable with, or even better than the existing alpha-decay systematics. The observed standard deviation (in a decimal logarithm scale) is around 0.38 for the complete set of alpha emitters, and around $\sigma = 0.28$ when the sub-set of even-even parent nuclei is taken into account. We have also demonstrated that even changing the inertial coefficient and the shape parametrization, among the combinations already used in previous papers [35–38], the values of the model parameters do not change significantly for the alpha decay process, as it is shown in tables

1 and 2. We have noted, however, some small deviation of our theoretical predictions from the experimental values for a few cases(mostly those located near the 126 neutron shell closure). This observation claims for improvement in the model to take into account the detailed quantum description of the potential barrier and the pre-formation probability of the alpha particle.

V. ACKNOWLEDGMENTS

The authors wish to express their gratitude to the Brazilian CNPq, CLAF, and FAPERJ for partial support.

---

[1] Gamow G 1928 *Z. Phys.* **51** 204; Condon E U and Gurney R W 1928 Nature **122** 439

[2] Sǎndulescu A and Greiner W 1992 *Rep. Prog. Phys.* **55** 1423

[3] Lazarev Yu A, Lobanov Yu V, Oganessian Yu Ts, Utyonkov V K, Abdullin F Sh, Polyakov A N, Rigol J, Shirokovsky I V, Tsyganov Yu S, Iliev S, Subbotin V G, Sukhov A M, Buklanov G V, Gikal B N, Kutner V B, Mezentsev A N, Subotic K, Wild J F, Lougheed R W and Moody K J 1996 *Phys. Rev.* C **54** 620

[4] Page R D, Woods P J, Cunningham R A, Davinson T, Davis N J, James A N, Livingston K, Sellin P J and Shotter A C 1996 *Phys. Rev.* C **53** 660

[5] Andreyev A N, Bijnens N, Enqvist T, Huyse M, Kuusiniemi P, Leino M, Trzaska W H, Uusitalo J and Van Duppen P 1997 *Z. Phys.* A **358** 63

[6] Leino M, Uusitalo J, Allatt R G, Armbruster P, Enqvist T, Eskola K, Hofmann S, Hurskanen S, Jokinen A, Ninov V, Page R D and Trzaska H 1996 *Z. Phys.* A **355** 157

[7] Liang C F, Paris P, Sheline R K, Alexa P and Gizon A 1996 *Phys. Rev.* C **54** 2304

[8] Wauters J, Batchelder J C, Bingham C R, Blumenthal D J, Brown L T, Conticchio L F, Davids C N, Davinson T, Irvine R J, Seweryniak D, Toth K S, Walters W B, Woods P J and Zganjar E F 1997 *Phys. Rev.* C **55** 1192

[9] Bingham C R, Toth K S, Batchelder J C, Blumenthal D J, Brown L T, Busse B C, Conticchio L F, Davids C N, Davinson T, Henderson D J, Irvine R J, Seweryniak D, Walters W B, Woods P J and Zimmerman B E 1996 *Phys. Rev.* C **54** R20

[10] Toth K S, Batchelder J C, Bingham C R, Conticchio L F, Walters W B, Davids C N, Henderson D J, Herman R, Penttilä H, Richards J D, Wuosmaa A H and Zimmerman B E 1996 *Phys. Rev.* C **53** 2513

[11] Enqvist T, Armbruster P, Eskola K, Leino M, Ninov V, Trzaska W H and Uusitalo J 1996 *Z. Phys.* A **354** 9

[12] Morita K, Pu Y H, Feng J, Hies M G, Lee K O, Yoshida A, Jeong S C, Kubono S, Nomura T, Tagaya Y, Wada M, Kurokawa M, Motobayashi T, Ogawa H, Uchibori T, Sueki K, Ishizuka T, Uchiyama K, Fujita Y, Miyatake H, Shimoda T, Shinozuka T, Kudo H, Nagai Y and Shin S A 1995 *Z. Phys.* A **352** 7

[13] Liang C F, Paris P, Plochocki A, Ruchowska E, Gizon A, Barnéoud D, Genevey J, Cãta G and Sheline R K 1996 *Z. Phys.* A **354** 153

[14] Bijnens N, Ahmad I, Andreyev A N, Batchelder J C, Bingham C R, Blumenthal D, Busse B C, Chen X S, Conticchio L F, Davids C N, Huyse M, Janssens R V F, Mantica P, Penttila H, Reviol W, Seweryniak D, Van Duppen P, Walters W B, Wauters J and Zimmerman B E 1996 *Z. Phys.* A **356** 3

[15] Schuurmans P, Will B, Berkes I, Camps J, De Jesus M, De Moor P, Herzog P, Lindroos M, Paulsen R,

Severijns N, Van Geert A, Van Duppen P, Vanneste L and NICOLE and ISOLDE Collaborations 1996 *Phys. Rev. Lett.* **77** 4720

[16] Hofmann S, Ninov V, Hessberger F P, Armbruster P, Folger H, Muenzenberg G, Schoett H J, Popeko A G, Yeremin A V, Andreyev A N, Saro S, Janik R and Leino M 1995 *Z. Phys.* A **350** 277

[17] Hofmann S, Ninov V, Hessberger F P, Armbruster P, Folger H, Muenzenberg G, Schoett H J, Popeko A G, Yeremin A V, Andreyev A N, Saro S, Janik R and Leino M 1995 *Z. Phys.* A **350** 281

[18] Hofmann S, Ninov V, Hessberger F P, Armbruster P, Folger H, Muenzenberg G, Schoett H J, Popeko A G, Yeremin A V, Saro S, Janik R and Leino M 1996 *Z. Phys.* A **354** 229

[19] Buck B, Merchant A C and Perez S M 1990 *Phys. Rev. C* **65** 2975; 1991 *J. Phys. G* **17** 1223

[20] Buck B, Merchant A C and Perez S M 1992 *Phys. Rev. C* **45** 2247

[21] Buck B, Merchant A C and Perez S M 1993 *Atom. Data Nucl. Data Tables* **54** 53

[22] Fröman P O 1957 *Mat. Fys. Sk. Dan. Vid. Selsk.* **1** 3

[23] Wapstra A H, Nijgh G J and Van Lieshout R 1959 in *Nuclear Spectroscopy Tables* (North-Holland, Amsterdam)

[24] Taagepera R and Nurmia M 1961 *Ann. Acad. Sci. Fenn. Ser. A* **78**

[25] Viola-Jr V E and Seaborg G T 1966 *J. Inorg. Nucl. Chem.* **28** 741

[26] Keller K A and Münzel H 1972 *Z. Phys.* **255** 419

[27] Hornshøj P, Hansen P G, Jonson B, Ravn H L, Westgaard L and Nielsen O N 1974 *Nucl. Phys. A* **230** 365

[28] Poenaru D N and Ivascu M 1983 *J. Physique* **44** 791

[29] Brown B A 1992 *Phys. Rev. C* **46** 811

[30] Delion D S and Liotta R J 1997 *Phys. Rev. C* **56** 1782

[31] Delion D S, Insolia A and Liotta R J 1992 *Phys. Rev. C* **46** 1346; 1993 *J. Phys. G.* **19** L189

[32] Insolia A, Curutchet P, Liotta R J and Delion D S 1991 *Phys. Rev. C* **44** 545

[33] Poenaru D N, Schnabel D, Greiner W, Mazilu D and Gherghescu R 1991 *Atom. Data Nucl. Data Tables* **48** 231

[34] Stewart T L, Kermode M W, Beachey D J, Rowley N, Grant I S and Kruppa A T 1996 *Phys. Rev. Lett.* **77** 36; 1996 *Nucl. Phys.* A **611** 332

[35] Gonçalves M and Duarte S B 1993 *Phys. Rev.* C **48** 2409

[36] Duarte S B and Gonçalves M G 1996 *Phys. Rev.* C **53** 2309

[37] Gonçalves M, Duarte S B, García F and Rodriguez O 1997 *Comp. Phys. Comm.* **107** 246

[38] Duarte S B, Rodriguez O, Tavares O A P, Gonçalves M, García F and Guzman F 1998 *Phys. Rev. C* **57** 2516

[39] Gonçalves M, Duarte S B and Tavares O A P 1997 *Phys. Rev. C* **56** 3414

[40] Poenaru D N, Maruhn J A, Greiner W, Ivascu M, Mazilu D and Ivascu I 1989 *Z. Phys.* A **333** 291

[41] Audi G, Bersillon O, Blachot J and Wapstra A H 1997 *Nucl. Phys.* A **624** 1

[42] Nuclear Data (NuDat) Retrieval Program, Generated at the National Nuclear Data Center, Brookhaven National Laboratory, Upton N.Y. (USA), March 1998

[43] Tuli J K Editor 1989-1997 *Nucl. Data Sheets* **56–82**; 1995 *Nuclear Wallet Cards* (Fifth Edition), National Nuclear Data Center, Brookhaven National Laboratory (Upton, N. Y.)

[44] Tavares O A P and Terranova M L *Radiat. Meas.* **27** 19

Table 1: The minima of σ from the family of curves $\sigma = \sigma(r_0,\ \lambda_0)$ (figure 1), and the mean values, $\bar{q}$, of the distributions in figure 2 according to the different model descriptions and inertia coefficients used to fit 349 alpha-decay half-life-values of ground-state to ground-state favoured alpha transitions; after data rejection in two runs, the final number of alpha-decay cases for all combinations of mass transfer and inertia was 324.

	Model description and inertia			
Quantity	Werner-Wheeler		Effective inertia	
	VMAS	CMAS	VMAS	CMAS
r_0 (fm)	1.34	1.20	1.13	1.13
λ_0 ($10^{22}\ s^{-1}$)	1.8	4.4	4.0	1.8
σ	0.38	0.38	0.38	0.38
$\bar{q}$	-0.001	-0.002	0.002	0.006

Table 2: The same as in Table 1, but for a total of 151 even-even alpha emitters. The corresponding $\log_{10}(\tau_c/\tau_e)$-distributions are shown in figure 3. In fitting the half-life data, only 8 cases have been rejected in two runs.

	Model description and inertia			
Quantity	Werner-Wheeler		Effective inertia	
	VMAS	CMAS	VMAS	CMAS
r_0 (fm)	1.35	1.21	1.15	1.15
λ_0 ($10^{22}\ s^{-1}$)	2.0	4.8	3.2	1.4
σ	0.30	0.29	0.28	0.28
$\bar{q}$	0.004	-0.002	-0.002	0.005

Table 3: Intercomparison between alpha-decay half-life-values calculated by the present models and the experimental data for 380 ground-state to ground-state favoured alpha transitions (model parameter-values are those of Table 1).

Half-life-values, τ (in seconds)

Parent nucleus		Present models				Experimental value
		Werner-Wheeler		Effective inertia		
A	Z	VMAS	CMAS	VMAS	CMAS	
106	52	.17E-03	.17E-03	.16E-03	.17E-03	.60E-04
107	52	.37E-02	.36E-02	.34E-02	.35E-02	.44E-02
108	52	.63E+01	.61E+01	.57E+01	.58E+01	.43E+01
109	52	.18E+03	.18E+03	.16E+03	.17E+03	.12E+03
110	52	.19E+07	.19E+07	.17E+07	.17E+07	.62E+06
108	53	.49E-02	.48E-02	.46E-02	.47E-02	.42E-01
110	53	.34E+01	.34E+01	.31E+01	.32E+01	.38E+01
111	53	.37E+03	.36E+03	.33E+03	.34E+03	.25E+04
112	53	.56E+05	.56E+05	.50E+05	.51E+05	.28E+06
113	53	.14E+08	.14E+08	.12E+08	.12E+08	.20E+10
111	54	.24E+01	.24E+01	.22E+01	.23E+01	.74E+00
112	54	.76E+03	.77E+03	.71E+03	.72E+03	.32E+03
113	54	.38E+05	.38E+05	.35E+05	.35E+05	.68E+04
114	55	.21E+04	.21E+04	.19E+04	.20E+04	.28E+04
144	60	.29E+24	.27E+24	.23E+24	.22E+24	.72E+23
145	61	.49E+18	.47E+18	.40E+18	.39E+18	.19E+18
146	62	.65E+16	.62E+16	.54E+16	.53E+16	.32E+16

147	62	.51E+19	.49E+19	.42E+19	.41E+19	.33E+19
148	62	.78E+24	.75E+24	.63E+24	.62E+24	.22E+24
147	63	.30E+12	.29E+12	.26E+12	.26E+12	.95E+11
148	63	.70E+14	.67E+14	.59E+14	.58E+14	.50E+15
148	64	.39E+10	.39E+10	.35E+10	.34E+10	.23E+10
149	64	.14E+12	.13E+12	.12E+12	.12E+12	.19E+12
150	64	.12E+15	.12E+15	.10E+15	.10E+15	.56E+14
151	64	.72E+16	.70E+16	.61E+16	.60E+16	.13E+16
152	64	.10E+23	.10E+23	.87E+22	.85E+22	.34E+22
150	66	.16E+04	.15E+04	.14E+04	.14E+04	.12E+04
151	66	.16E+05	.15E+05	.14E+05	.14E+05	.19E+05
152	66	.17E+08	.17E+08	.16E+08	.16E+08	.86E+07
153	66	.31E+09	.30E+09	.28E+09	.27E+09	.24E+09
154	66	.12E+15	.12E+15	.10E+15	.10E+15	.95E+14
152	67	.63E+03	.63E+03	.60E+03	.60E+03	.13E+04
154	67	.43E+06	.43E+06	.40E+06	.40E+06	.35E+07
152	68	.14E+02	.15E+02	.14E+02	.14E+02	.11E+02
153	68	.64E+02	.64E+02	.61E+02	.62E+02	.70E+02
154	68	.54E+05	.55E+05	.52E+05	.52E+05	.48E+05
155	68	.54E+06	.55E+06	.51E+06	.51E+06	.16E+07
156	68	.57E+11	.58E+11	.53E+11	.53E+11	.23E+11
155	69	.38E+04	.39E+04	.37E+04	.37E+04	.11E+04

156	69	.77E+05	.78E+05	.75E+05	.74E+05	.14E+06
154	70	.52E+00	.54E+00	.53E+00	.54E+00	.44E+00
155	70	.17E+01	.17E+01	.17E+01	.17E+01	.20E+01
156	70	.70E+03	.72E+03	.70E+03	.70E+03	.26E+03
157	70	.64E+04	.66E+04	.64E+04	.64E+04	.77E+04
158	70	.36E+07	.37E+07	.35E+07	.35E+07	.46E+07
158	71	.30E+04	.31E+04	.30E+04	.30E+04	.12E+04
159	71	.14E+06	.14E+06	.14E+06	.14E+06	.30E+05
160	71	.38E+08	.40E+08	.38E+08	.37E+08	≥.36E+08
156	72	.21E-01	.23E-01	.23E-01	.23E-01	.25E-01
157	72	.79E-01	.83E-01	.84E-01	.85E-01	.13E+00
158	72	.84E+01	.89E+01	.88E+01	.89E+01	.65E+01
159	72	.63E+02	.66E+02	.65E+02	.65E+02	.14E+02
160	72	.22E+04	.23E+04	.23E+04	.23E+04	.19E+04
161	72	.23E+05	.24E+05	.23E+05	.23E+05	.58E+04
162	72	.13E+07	.13E+07	.13E+07	.13E+07	.49E+06
174	72	.18E+25	.18E+25	.16E+25	.15E+25	.63E+23
157	73	.30E-02	.32E-02	.33E-02	.34E-02	<.53E-02
158	73	.13E-01	.14E-01	.14E-01	.14E-01	.40E-01
159	73	.20E+01	.21E+01	.22E+01	.22E+01	.71E+00
160	73	.16E+02	.17E+02	.17E+02	.18E+02	.46E+01
161	73	.98E+02	.10E+03	.10E+03	.10E+03	.60E+02
162	73	.21E+04	.22E+04	.22E+04	.22E+04	.45E+04
163	73	.46E+05	.48E+05	.47E+05	.47E+05	.55E+04

158	74	.15E-02	.16E-02	.17E-02	.17E-02	.90E-03
159	74	.48E-02	.52E-02	.54E-02	.54E-02	.73E-02
160	74	.11E+00	.12E+00	.12E+00	.12E+00	.10E+00
161	74	.46E+00	.49E+00	.50E+00	.51E+00	.50E+00
162	74	.45E+01	.48E+01	.49E+01	.49E+01	.30E+01
163	74	.20E+02	.21E+02	.21E+02	.21E+02	.67E+01
164	74	.29E+03	.30E+03	.30E+03	.30E+03	.25E+01
165	74	.45E+04	.47E+04	.47E+04	.47E+04	>.25E+04
166	74	.40E+05	.42E+05	.41E+05	.41E+05	.47E+05
168	74	.42E+07	.44E+07	.42E+07	.42E+07	.16E+07

160	75	.17E-02	.19E-02	.20E-02	.20E-02	.88E-02
161	75	.14E-01	.15E-01	.15E-01	.16E-01	.15E-01
162	75	.51E-01	.55E-01	.57E-01	.57E-01	<.33E+01
163	75	.50E+00	.54E+00	.55E+00	.56E+00	.41E+00
164	75	.11E+01	.12E+01	.12E+01	.12E+01	.15E+01
165	75	.39E+02	.42E+02	.42E+02	.42E+02	.18E+02
167	75	.11E+04	.11E+04	.11E+04	.11E+04	.62E+03
169	75	.13E+05	.14E+05	.14E+05	.14E+05	.81E+07

162	76	.22E-02	.24E-02	.25E-02	.25E-02	.19E-02
164	76	.24E-01	.26E-01	.27E-01	.28E-01	.42E-01
165	76	.84E-01	.90E-01	.93E-01	.94E-01	<.12E+00
166	76	.44E+00	.47E+00	.48E+00	.48E+00	.27E+00
167	76	.19E+01	.20E+01	.20E+01	.20E+01	.12E+01
168	76	.76E+01	.81E+01	.82E+01	.82E+01	.45E+01
169	76	.22E+02	.23E+02	.23E+02	.23E+02	.31E+02

170	76	.13E+03	.14E+03	.14E+03	.14E+03	.61E+02
171	76	.85E+03	.89E+03	.89E+03	.89E+03	.47E+03
172	76	.41E+04	.43E+04	.42E+04	.42E+04	.96E+04
173	76	.27E+05	.28E+05	.27E+05	.27E+05	.80E+05
174	76	.28E+06	.29E+06	.29E+06	.29E+06	.22E+06
186	76	.61E+23	.61E+23	.54E+23	.53E+23	.63E+23
166	77	.95E-02	.10E-01	.11E-01	.11E-01	>.50E-02
167	77	.51E-01	.55E-01	.58E-01	.58E-01	≥.50E-02
169	77	.32E+00	.34E+00	.35E+00	.35E+00	.40E+00
170	77	.75E+00	.80E+00	.82E+00	.82E+00	.14E+01
171	77	.86E+00	.91E+00	.93E+00	.94E+00	.15E+01
175	77	.53E+02	.55E+02	.55E+02	.55E+02	.11E+04
176	77	.10E+05	.11E+05	.11E+05	.11E+05	.38E+03
177	77	.37E+05	.38E+05	.38E+05	.38E+05	.50E+05
169	78	.81E-02	.87E-02	.92E-02	.93E-02	.25E-02
170	78	.22E-01	.24E-01	.25E-01	.25E-01	.60E-02
171	78	.48E-01	.51E-01	.54E-01	.54E-01	.25E-01
172	78	.15E+00	.16E+00	.17E+00	.17E+00	.11E+00
173	78	.38E+00	.40E+00	.41E+00	.42E+00	.41E+00
174	78	.17E+01	.18E+01	.19E+01	.19E+01	.11E+01
176	78	.28E+02	.29E+02	.30E+02	.30E+02	.17E+02
177	78	.36E+03	.37E+03	.38E+03	.38E+03	.20E+03
178	78	.65E+03	.68E+03	.68E+03	.68E+03	.27E+03
180	78	.21E+05	.21E+05	.21E+05	.21E+05	.17E+05
181	78	.74E+05	.77E+05	.75E+05	.75E+05	.85E+05
183	78	.56E+07	.58E+07	.56E+07	.55E+07	.30E+08

184	78	.11E+09	.11E+09	.10E+09	.10E+09	.10E+09
186	78	.74E+10	.75E+10	.71E+10	.70E+10	.53E+10
188	78	.15E+13	.16E+13	.14E+13	.14E+13	.34E+13
190	78	.14E+20	.14E+20	.13E+20	.13E+20	.10E+20

172	79	.44E-02	.47E-02	.50E-02	.50E-02	≥.40E-05
173	79	.26E-01	.28E-01	.29E-01	.29E-01	≥.59E-01
174	79	.27E-01	.28E-01	.30E-01	.30E-01	<.12E+00
175	79	.63E-01	.67E-01	.70E-01	.70E-01	.21E+00
179	79	.12E+02	.12E+02	.12E+02	.12E+02	.32E+02
180	79	.99E+02	.10E+03	.10E+03	.10E+03	≤.45E+03
183	79	.58E+04	.60E+04	.60E+04	.60E+04	.12E+05
185	79	.15E+06	.15E+06	.15E+06	.15E+06	.98E+05

175	80	.88E-02	.95E-02	.10E-01	.10E-01	.20E-01
176	80	.22E-01	.23E-01	.25E-01	.25E-01	.34E-01
177	80	.97E-01	.10E+00	.11E+00	.11E+00	.15E+00
178	80	.35E+00	.38E+00	.39E+00	.40E+00	.36E+00
179	80	.12E+01	.13E+01	.13E+01	.13E+01	.21E+01
180	80	.54E+01	.57E+01	.59E+01	.59E+01	.61E+01
182	80	.67E+02	.71E+02	.72E+02	.72E+02	.71E+02
183	80	.43E+02	.45E+02	.46E+02	.46E+02	.37E+02
184	80	.19E+04	.20E+04	.20E+04	.20E+04	.28E+04
185	80	.57E+03	.59E+03	.59E+03	.59E+03	.82E+03
188	80	.26E+09	.26E+09	.26E+09	.25E+09	.53E+09
190	80	.71E+14	.74E+14	.70E+14	.69E+14	>.24E+10

179	81	.13E+00	.14E+00	.15E+00	.15E+00	.16E+00

182	81	.10E+01	.11E+01	.11E+01	.11E+01	>.77E+02
183	81	.20E+02	.22E+02	.22E+02	.22E+02	>.60E+00
186	81	.48E+03	.51E+03	.51E+03	.51E+03	.46E+06
181	82	.10E-01	.11E-01	.12E-01	.12E-01	>.45E-01
182	82	.37E-01	.40E-01	.42E-01	.42E-01	.55E-01
183	82	.53E-01	.56E-01	.60E-01	.60E-01	.32E+00
184	82	.40E+00	.42E+00	.45E+00	.45E+00	<.55E+00
186	82	.51E+01	.54E+01	.56E+01	.56E+01	.10E+02
188	82	.14E+03	.15E+03	.16E+03	.16E+03	.11E+03
189	82	.18E+04	.19E+04	.19E+04	.19E+04	.13E+05
192	82	.31E+07	.32E+07	.32E+07	.32E+07	.37E+07
194	82	.21E+10	.22E+10	.21E+10	.21E+10	.99E+10
196	82	.73E+13	.75E+13	.72E+13	.71E+13	≥.74E+10
210	82	.17E+17	.16E+17	.14E+17	.14E+17	.37E+17
190	84	.26E-02	.28E-02	.30E-02	.30E-02	.24E-02
191	84	.82E-02	.85E-02	.91E-02	.92E-02	.15E-01
192	84	.26E-01	.27E-01	.29E-01	.29E-01	.34E-01
193	84	.14E+00	.15E+00	.16E+00	.16E+00	.26E+00
194	84	.31E+00	.32E+00	.34E+00	.34E+00	.39E+00
195	84	.25E+01	.26E+01	.27E+01	.27E+01	.62E+01
196	84	.54E+01	.55E+01	.57E+01	.57E+01	.59E+01
197	84	.52E+02	.53E+02	.54E+02	.55E+02	.12E+03
198	84	.13E+03	.13E+03	.13E+03	.14E+03	.18E+03
199	84	.13E+04	.13E+04	.13E+04	.13E+04	.44E+04

200	84	.31E+04	.31E+04	.31E+04	.31E+04	.62E+04
201	84	.21E+05	.21E+05	.21E+05	.21E+05	.57E+05
202	84	.69E+05	.69E+05	.68E+05	.68E+05	.14E+06
203	84	.69E+06	.69E+06	.68E+06	.68E+06	.20E+07
204	84	.75E+06	.75E+06	.73E+06	.73E+06	.19E+07
205	84	.55E+07	.55E+07	.53E+07	.53E+07	.15E+08
206	84	.49E+07	.49E+07	.47E+07	.47E+07	.14E+08
207	84	.20E+08	.19E+08	.19E+08	.18E+08	.10E+09
208	84	.19E+08	.19E+08	.18E+08	.18E+08	.91E+08
210	84	.15E+07	.15E+07	.14E+07	.14E+07	.12E+08
212	84	.26E-06	.22E-06	.23E-06	.24E-06	.30E-06
213	84	.28E-05	.24E-05	.25E-05	.26E-05	.42E-05
214	84	.25E-03	.22E-03	.22E-03	.23E-03	.16E-03
215	84	.22E-02	.19E-02	.19E-02	.19E-02	.18E-03
216	84	.27E+00	.25E+00	.24E+00	.24E+00	.15E+00
217	84	.21E+01	.19E+01	.18E+01	.19E+01	<.10E+02
218	84	.40E+03	.36E+03	.33E+03	.34E+03	.19E+03

194	85	.64E-01	.67E-01	.71E-01	.72E-01	.40E-01
196	85	.14E+00	.15E+00	.15E+00	.16E+00	.25E+00
197	85	.30E+00	.31E+00	.33E+00	.33E+00	.36E+00
198	85	.17E+01	.17E+01	.18E+01	.18E+01	.47E+01
199	85	.46E+01	.47E+01	.49E+01	.49E+01	.80E+01
201	85	.66E+02	.67E+02	.68E+02	.69E+02	.12E+03
203	85	.77E+03	.78E+03	.78E+03	.79E+03	.14E+04
204	85	.35E+04	.35E+04	.35E+04	.35E+04	.14E+05
205	85	.56E+04	.56E+04	.56E+04	.56E+04	.16E+05
207	85	.24E+05	.24E+05	.24E+05	.24E+05	.75E+05

208	85	.91E+05	.90E+05	.88E+05	.88E+05	.11E+07
209	85	.82E+05	.80E+05	.78E+05	.78E+05	.47E+06
211	85	.63E+04	.61E+04	.59E+04	.60E+04	.62E+05
213	85	.11E-06	.95E-07	.10E-06	.10E-06	.12E-06
214	85	.45E-06	.40E-06	.41E-06	.43E-06	.56E-06
215	85	.58E-04	.52E-04	.53E-04	.55E-04	.10E-03
216	85	.26E-03	.23E-03	.23E-03	.24E-03	.30E-03
217	85	.63E-01	.57E-01	.56E-01	.57E-01	.32E-01
219	85	.77E+02	.70E+02	.66E+02	.68E+02	.58E+02
220	85	.23E+04	.21E+04	.20E+04	.20E+04	.28E+04

196	86	.15E-01	.15E-01	.16E-01	.17E-01	<.30E-02
197	86	.68E-01	.71E-01	.76E-01	.77E-01	.65E-01
199	86	.59E+00	.61E+00	.64E+00	.65E+00	.66E+00
200	86	.12E+01	.12E+01	.13E+01	.13E+01	.11E+01
201	86	.54E+01	.55E+01	.58E+01	.58E+01	.87E+01
202	86	.11E+02	.12E+02	.12E+02	.12E+02	.11E+02
203	86	.43E+02	.44E+02	.45E+02	.45E+02	.68E+02
204	86	.87E+02	.88E+02	.90E+02	.91E+02	.10E+03
206	86	.37E+03	.37E+03	.38E+03	.38E+03	.55E+03
207	86	.14E+04	.14E+04	.15E+04	.15E+04	.26E+04
208	86	.12E+04	.12E+04	.12E+04	.12E+04	.24E+04
209	86	.33E+04	.33E+04	.33E+04	.33E+04	.10E+05
210	86	.31E+04	.30E+04	.30E+04	.30E+04	.90E+04
212	86	.29E+03	.28E+03	.28E+03	.28E+03	.14E+04
214	86	.30E-06	.27E-06	.28E-06	.29E-06	.27E-06
215	86	.23E-05	.21E-05	.22E-05	.23E-05	.23E-05
216	86	.12E-03	.11E-03	.11E-03	.11E-03	.45E-04

217	86	.95E-03	.86E-03	.87E-03	.89E-03	.54E-03
218	86	.98E-01	.90E-01	.89E-01	.91E-01	.35E-01
220	86	.18E+03	.16E+03	.16E+03	.16E+03	.56E+02
222	86	.11E+07	.10E+07	.97E+06	.98E+06	.33E+06
200	87	.32E-01	.33E-01	.35E-01	.36E-01	.19E-01
201	87	.60E-01	.62E-01	.67E-01	.67E-01	.48E-01
202	87	.19E+00	.19E+00	.20E+00	.20E+00	.35E+00
203	87	.39E+00	.40E+00	.43E+00	.43E+00	.58E+00
204	87	.10E+01	.10E+01	.11E+01	.11E+01	.21E+01
205	87	.24E+01	.25E+01	.26E+01	.26E+01	.39E+01
206	87	.72E+01	.73E+01	.76E+01	.76E+01	.19E+02
207	87	.89E+01	.90E+01	.93E+01	.94E+01	.16E+02
208	87	.25E+02	.25E+02	.26E+02	.26E+02	.66E+02
209	87	.22E+02	.22E+02	.23E+02	.23E+02	.56E+02
211	87	.63E+02	.62E+02	.63E+02	.64E+02	<.23E+03
213	87	.65E+01	.63E+01	.63E+01	.64E+01	.35E+02
215	87	.11E-06	.96E-07	.10E-06	.11E-06	.86E-07
216	87	.75E-06	.67E-06	.71E-06	.74E-06	.70E-06
217	87	.48E-04	.44E-04	.45E-04	.47E-04	.16E-04
218	87	.94E-03	.86E-03	.88E-03	.91E-03	.11E-02
219	87	.57E-01	.53E-01	.53E-01	.54E-01	.20E-01
220	87	.13E+02	.12E+02	.11E+02	.12E+02	.42E+02
223	87	.25E+08	.23E+08	.22E+08	.22E+08	.22E+08
203	88	.32E-01	.33E-01	.35E-01	.36E-01	.10E-02
204	88	.64E-01	.66E-01	.71E-01	.72E-01	.59E-01
206	88	.33E+00	.33E+00	.35E+00	.36E+00	.24E+00

207	88	.97E+00	.99E+00	.10E+01	.11E+01	.14E+01
208	88	.10E+01	.10E+01	.11E+01	.11E+01	.14E+01
209	88	.26E+01	.27E+01	.28E+01	.28E+01	.51E+01
210	88	.21E+01	.21E+01	.22E+01	.23E+01	.38E+01
211	88	.57E+01	.57E+01	.59E+01	.59E+01	<.14E+02
212	88	.62E+01	.61E+01	.63E+01	.64E+01	.14E+02
214	88	.74E+00	.73E+00	.75E+00	.76E+00	.25E+01
216	88	.25E-06	.23E-06	.24E-06	.25E-06	.18E-06
217	88	.18E-05	.16E-05	.17E-05	.18E-05	.17E-05
218	88	.67E-04	.62E-04	.65E-04	.67E-04	.26E-04
220	88	.46E-01	.43E-01	.44E-01	.45E-01	.18E-01
222	88	.98E+02	.92E+02	.91E+02	.92E+02	.39E+02
224	88	.10E+07	.96E+06	.92E+06	.93E+06	.33E+06
226	88	.20E+12	.19E+12	.18E+12	.18E+12	.53E+11
207	89	.26E-01	.27E-01	.29E-01	.29E-01	.22E-01
208	89	.71E-01	.73E-01	.78E-01	.79E-01	.96E-01
209	89	.68E-01	.69E-01	.74E-01	.75E-01	.10E+00
210	89	.16E+00	.17E+00	.18E+00	.18E+00	.36E+00
211	89	.13E+00	.14E+00	.14E+00	.15E+00	.25E+00
212	89	.28E+00	.28E+00	.30E+00	.30E+00	.96E+00
213	89	.34E+00	.34E+00	.36E+00	.36E+00	.80E+00
215	89	.45E-01	.44E-01	.46E-01	.47E-01	.17E+00
217	89	.11E-06	.97E-07	.11E-06	.11E-06	.69E-07
218	89	.11E-05	.10E-05	.11E-05	.12E-05	.11E-05
219	89	.26E-04	.24E-04	.26E-04	.26E-04	.12E-04
222	89	.46E+01	.43E+01	.44E+01	.45E+01	.54E+01

210	90	.15E-01	.15E-01	.16E-01	.17E-01	.90E-02
212	90	.28E-01	.28E-01	.30E-01	.31E-01	.30E-01
213	90	.65E-01	.65E-01	.70E-01	.71E-01	.14E+00
214	90	.67E-01	.67E-01	.72E-01	.73E-01	.10E+00
216	90	.10E-01	.10E-01	.11E-01	.11E-01	.28E-01
218	90	.20E-06	.19E-06	.21E-06	.21E-06	.11E-06
219	90	.11E-05	.11E-05	.12E-05	.12E-05	.11E-05
220	90	.27E-04	.26E-04	.28E-04	.29E-04	.97E-05
222	90	.54E-02	.51E-02	.54E-02	.55E-02	.28E-02
224	90	.28E+01	.26E+01	.27E+01	.27E+01	.13E+01
226	90	.64E+04	.61E+04	.61E+04	.62E+04	.24E+04
228	90	.25E+09	.24E+09	.23E+09	.23E+09	.83E+08
230	90	.12E+14	.11E+14	.11E+14	.11E+14	.31E+13
232	90	.29E+19	.28E+19	.26E+19	.26E+19	.57E+18

213	91	.30E-02	.31E-02	.34E-02	.34E-02	.53E-02
214	91	.66E-02	.67E-02	.73E-02	.74E-02	≥.17E-01
215	91	.78E-02	.78E-02	.85E-02	.87E-02	.15E-01
216	91	.22E-01	.22E-01	.23E-01	.24E-01	.29E+00
217	91	.13E-02	.13E-02	.14E-02	.14E-02	.34E-02
218	91	.58E-06	.55E-06	.61E-06	.63E-06	.18E-03
219	91	.12E-06	.12E-06	.13E-06	.14E-06	.53E-07
220	91	.44E-06	.42E-06	.46E-06	.48E-06	.78E-06
221	91	.10E-04	.98E-05	.11E-04	.11E-04	.59E-05
224	91	.31E+00	.30E+00	.31E+00	.32E+00	.79E+00
225	91	.33E+01	.32E+01	.33E+01	.34E+01	.24E+01
227	91	.49E+04	.48E+04	.48E+04	.49E+04	.54E+04

218	92	.46E-03	.45E-03	.50E-03	.51E-03	.15E-02
222	92	.56E-05	.53E-05	.59E-05	.61E-05	.10E-05
223	92	.15E-03	.14E-03	.15E-03	.16E-03	.18E-04
224	92	.10E-02	.10E-02	.11E-02	.11E-02	.90E-03
225	92	.66E-01	.64E-01	.68E-01	.69E-01	.10E+00
226	92	.63E+00	.62E+00	.65E+00	.66E+00	.20E+00
228	92	.15E+04	.15E+04	.15E+04	.16E+04	<.57E+03
229	92	.38E+05	.38E+05	.38E+05	.38E+05	.27E+05
230	92	.73E+07	.72E+07	.72E+07	.72E+07	.27E+07
232	92	.98E+10	.97E+10	.94E+10	.94E+10	.32E+10
233	92	.16E+14	.15E+14	.15E+14	.15E+14	.59E+13
234	92	.33E+14	.33E+14	.31E+14	.31E+14	.11E+14
236	92	.39E+16	.38E+16	.36E+16	.35E+16	.10E+16
238	92	.99E+18	.96E+18	.89E+18	.89E+18	.18E+18
225	93	.82E-03	.79E-03	.87E-03	.89E-03	>.20E-05
226	93	.44E-01	.43E-01	.46E-01	.47E-01	.70E-01
227	93	.72E+00	.70E+00	.75E+00	.76E+00	.51E+00
228	93	.18E+02	.17E+02	.18E+02	.18E+02	.15E+03
229	93	.63E+03	.62E+03	.64E+03	.65E+03	<.46E+03
230	93	.53E+04	.52E+04	.53E+04	.54E+04	≤.92E+04
231	93	.34E+06	.33E+06	.34E+06	.34E+06	.15E+06
228	94	.64E+00	.64E+00	.69E+00	.70E+00	.20E+00
229	94	.99E+01	.99E+01	.10E+02	.11E+02	>.20E-05
230	94	.35E+03	.35E+03	.37E+03	.37E+03	≥.20E+03
232	94	.25E+05	.25E+05	.26E+05	.26E+05	.16E+05

233	94	.54E+06	.54E+06	.55E+06	.56E+06	.10E+07
234	94	.16E+07	.16E+07	.16E+07	.16E+07	.53E+06
235	94	.96E+08	.96E+08	.96E+08	.96E+08	.56E+08
236	94	.26E+09	.25E+09	.25E+09	.25E+09	.13E+09
238	94	.78E+10	.77E+10	.76E+10	.76E+10	.39E+10
239	94	.96E+12	.95E+12	.92E+12	.92E+12	.10E+13
240	94	.79E+12	.77E+12	.75E+12	.75E+12	.28E+12
242	94	.45E+14	.44E+14	.42E+14	.42E+14	.15E+14
244	94	.83E+16	.81E+16	.76E+16	.76E+16	.32E+16

232	95	.36E+03	.36E+03	.38E+03	.39E+03	.39E+04
237	95	.18E+08	.18E+08	.18E+08	.18E+08	.15E+08

238	96	.45E+06	.45E+06	.47E+06	.47E+06	≥.86E+05
240	96	.44E+07	.44E+07	.45E+07	.45E+07	.33E+07
242	96	.31E+08	.31E+08	.31E+08	.31E+08	.19E+08
244	96	.12E+10	.12E+10	.12E+10	.12E+10	.75E+09
246	96	.32E+12	.32E+12	.31E+12	.31E+12	.18E+12
248	96	.30E+14	.29E+14	.28E+14	.28E+14	.14E+14
250	96	.24E+14	.24E+14	.22E+14	.23E+14	.28E+13

240	98	.10E+03	.10E+03	.11E+03	.11E+03	.64E+02
242	98	.52E+03	.52E+03	.55E+03	.56E+03	.26E+03
244	98	.28E+04	.27E+04	.29E+04	.29E+04	.15E+04
246	98	.22E+06	.22E+06	.23E+06	.23E+06	.16E+06
248	98	.44E+08	.43E+08	.44E+08	.44E+08	.35E+08
250	98	.61E+09	.60E+09	.60E+09	.61E+09	.49E+09
252	98	.20E+09	.19E+09	.19E+09	.19E+09	.10E+09

254	98	.63E+10	.61E+10	.60E+10	.60E+10	.20E+10
256	98	.82E+12	.79E+12	.76E+12	.77E+12	.74E+11
251	99	.86E+07	.84E+07	.86E+07	.87E+07	.30E+08
253	99	.17E+07	.17E+07	.17E+07	.17E+07	.20E+07
245	100	.20E+01	.20E+01	.22E+01	.22E+01	.42E+01
246	100	.32E+01	.32E+01	.35E+01	.36E+01	.12E+01
248	100	.51E+02	.50E+02	.54E+02	.55E+02	.45E+02
250	100	.20E+04	.20E+04	.21E+04	.22E+04	<.20E+04
252	100	.79E+05	.77E+05	.81E+05	.82E+05	.11E+06
254	100	.17E+05	.16E+05	.17E+05	.17E+05	.14E+05
256	100	.23E+06	.22E+06	.23E+06	.23E+06	.14E+06
247	101	.14E+00	.14E+00	.16E+00	.16E+00	.29E+01
259	101	.25E+06	.24E+06	.25E+06	.25E+06	>.19E+06
260	101	.13E+07	.12E+07	.13E+07	.13E+07	>.96E+07
250	102	.23E+00	.23E+00	.25E+00	.26E+00	.50E+00
252	102	.39E+01	.39E+01	.43E+01	.43E+01	.42E+01
254	102	.44E+02	.43E+02	.47E+02	.47E+02	.72E+02
256	102	.27E+01	.26E+01	.28E+01	.29E+01	.36E+01
258	102	.70E+02	.67E+02	.72E+02	.74E+02	.12E+03
252	103	.14E+00	.13E+00	.15E+00	.16E+00	.11E+01
253	104	.22E-01	.22E-01	.25E-01	.26E-01	.36E+01
254	104	.63E-01	.63E-01	.72E-01	.73E-01	.17E+00

256	104	.10E+01	.10E+01	.12E+01	.12E+01	.36E+00
258	104	.75E-01	.73E-01	.82E-01	.84E-01	.11E+00
260	104	.13E+01	.13E+01	.14E+01	.15E+01	.10E+01
255	105	.16E-01	.16E-01	.18E-01	.19E-01	.20E+01
256	105	.70E-01	.70E-01	.81E-01	.82E-01	≥.29E+01
261	105	.31E+00	.30E+00	.34E+00	.35E+00	<.36E+01
260	106	.79E-02	.77E-02	.90E-02	.92E-02	.85E-02
265	106	.22E+01	.21E+01	.24E+01	.24E+01	≤.32E+02
264	108	.68E-03	.67E-03	.80E-03	.82E-03	.10E-03
265	108	.15E-02	.15E-02	.18E-02	.18E-02	.18E-02
266	109	.11E-04	.11E-04	.13E-04	.14E-04	.34E-02
269	110	.81E-05	.77E-05	.95E-05	.99E-05	.17E-03
272	111	.15E-03	.14E-03	.17E-03	.18E-03	≥.15E-02

Figure captions:

Figure 1: Variation of the root-mean-square of the quantity $q = \log_{10}(\tau_c/\tau_e)$, σ (equation 18), with the model parameter λ_0, for different values of nuclear radius parameter, r_0. τ_c is the calculated half-life, and τ_e is the experimental one. The figure shows the results for the combination of mass transfer VMAS with the effective inertia, μ_{eff}^{VMAS}, in obtaining τ_c values. A total of $N = 324$ alpha-decay half-life-values have been used in constructing each curve.

Figure 2: Distribution of the quantity $\log_{10}(\tau_c/\tau_e)$ at the minimum σ-value and with the correspondent best values of parameters r_0 and λ_0 listed in Table 1. The mean value, $\bar{q}$ (equation 19), of each distribution is very close to 0 (see table 1). The model combination is as follows: μ_{WW}^{VMAS} in part (a); μ_{WW}^{CMAS} in (b); μ_{eff}^{VMAS} in (c); and μ_{eff}^{CMAS} in (d).

Figure 3: The same as in figure 2, but for the sub-set of 151 even-even alpha emitters. Best r_0- and λ_0-values obtained in minimizing σ (equation 18) are listed in Table 2.

Figure 4: The ratio τ_c/τ_e (in $\log_{10}$-scale) of calculated to experimental alpha-decay half-life (points) is plotted versus neutron number of the parent nucleus; the full lines connect points for parent nuclei of a given proton number. Deviation by a factor of 3 between theory and experiment is represented by dashed lines. The figure shows the results for the model combination μ_{eff}^{VMAS}, and $N = 324$ alpha emitters (see Table 1).

Figure 5: The same as in figure 4, but for a sub-set of $N = 151$ even-even alpha emitters (see Table 2).

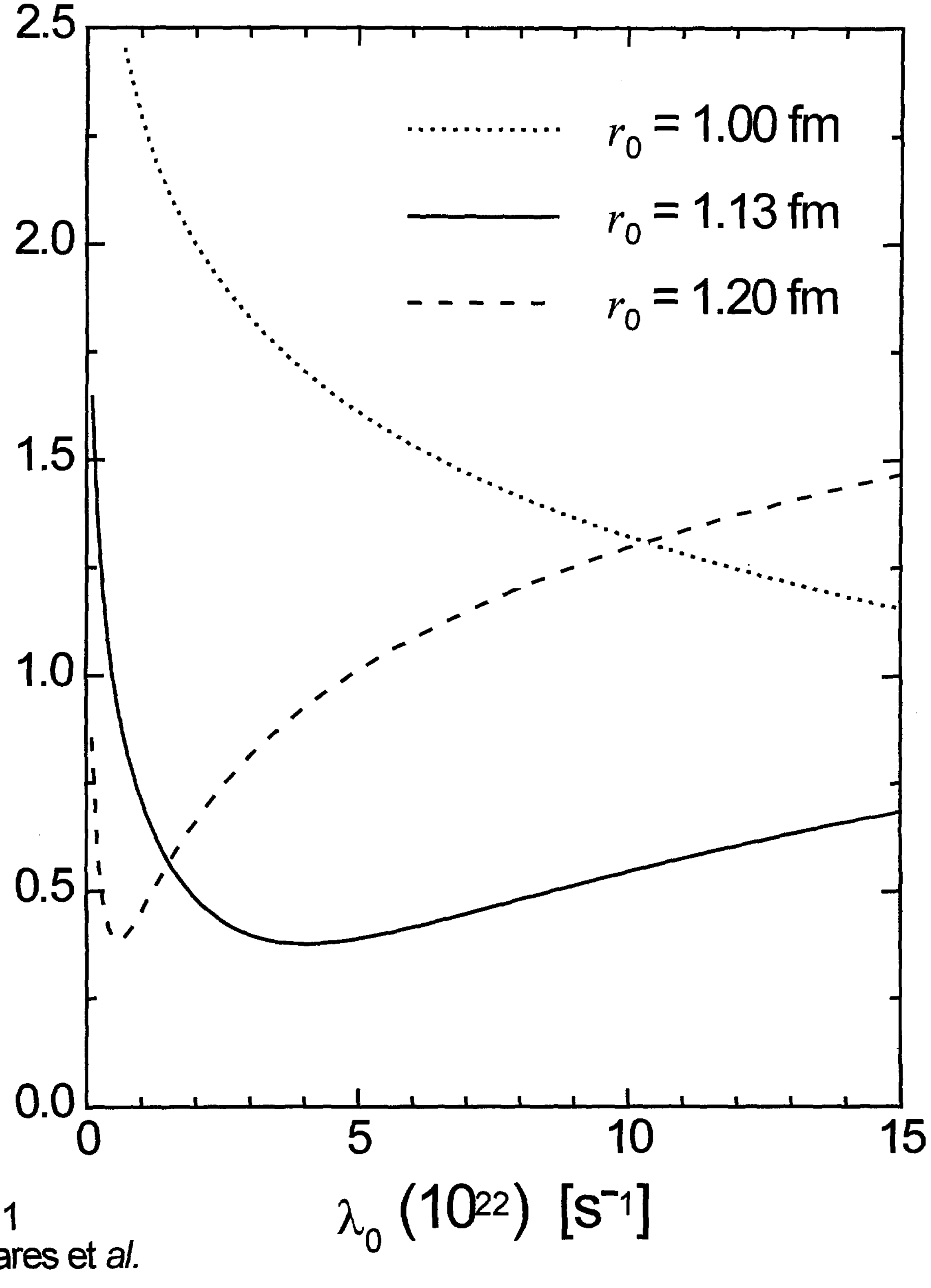

Fig. 1
Tavares et *al.*

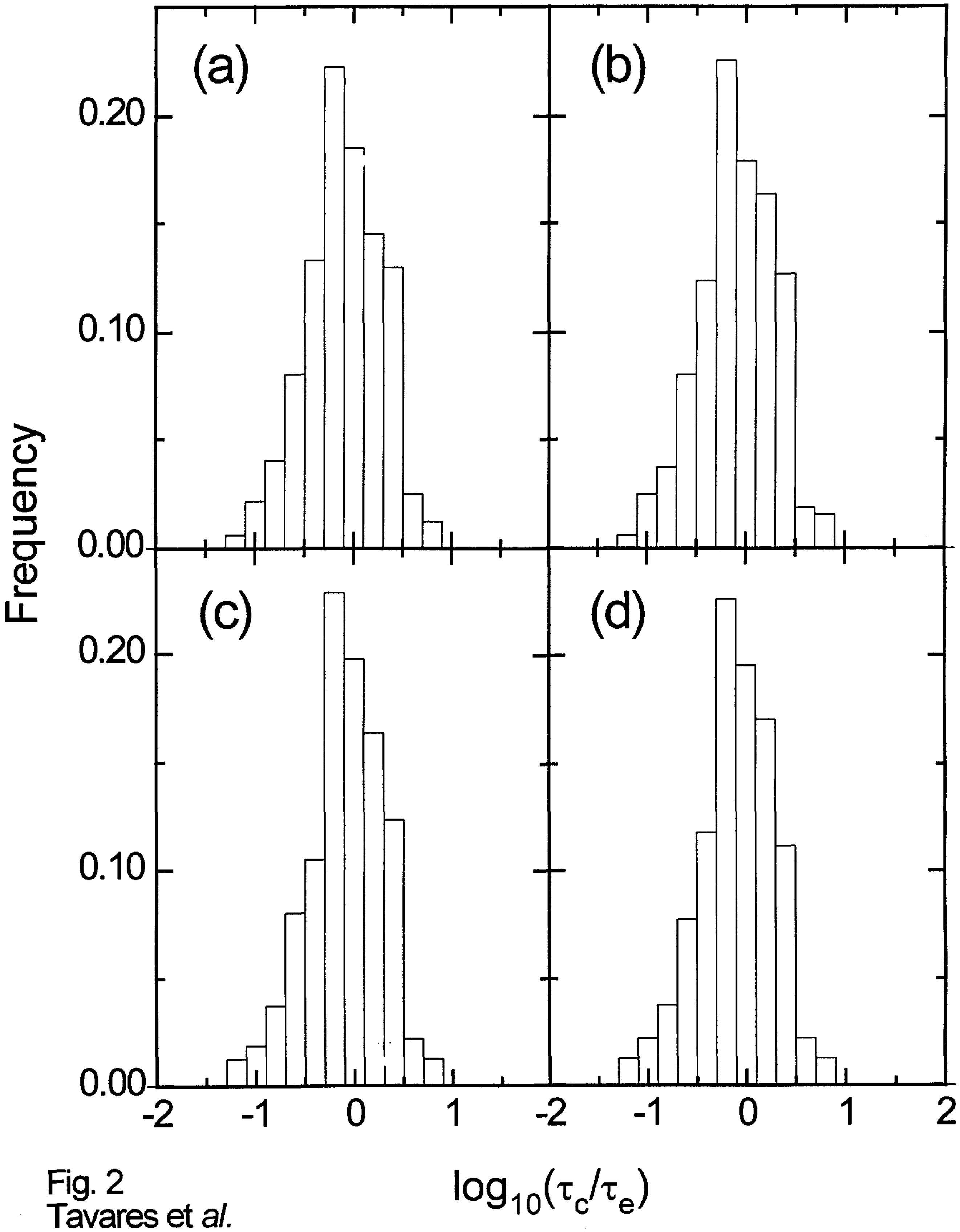

Fig. 2
Tavares et *al.*

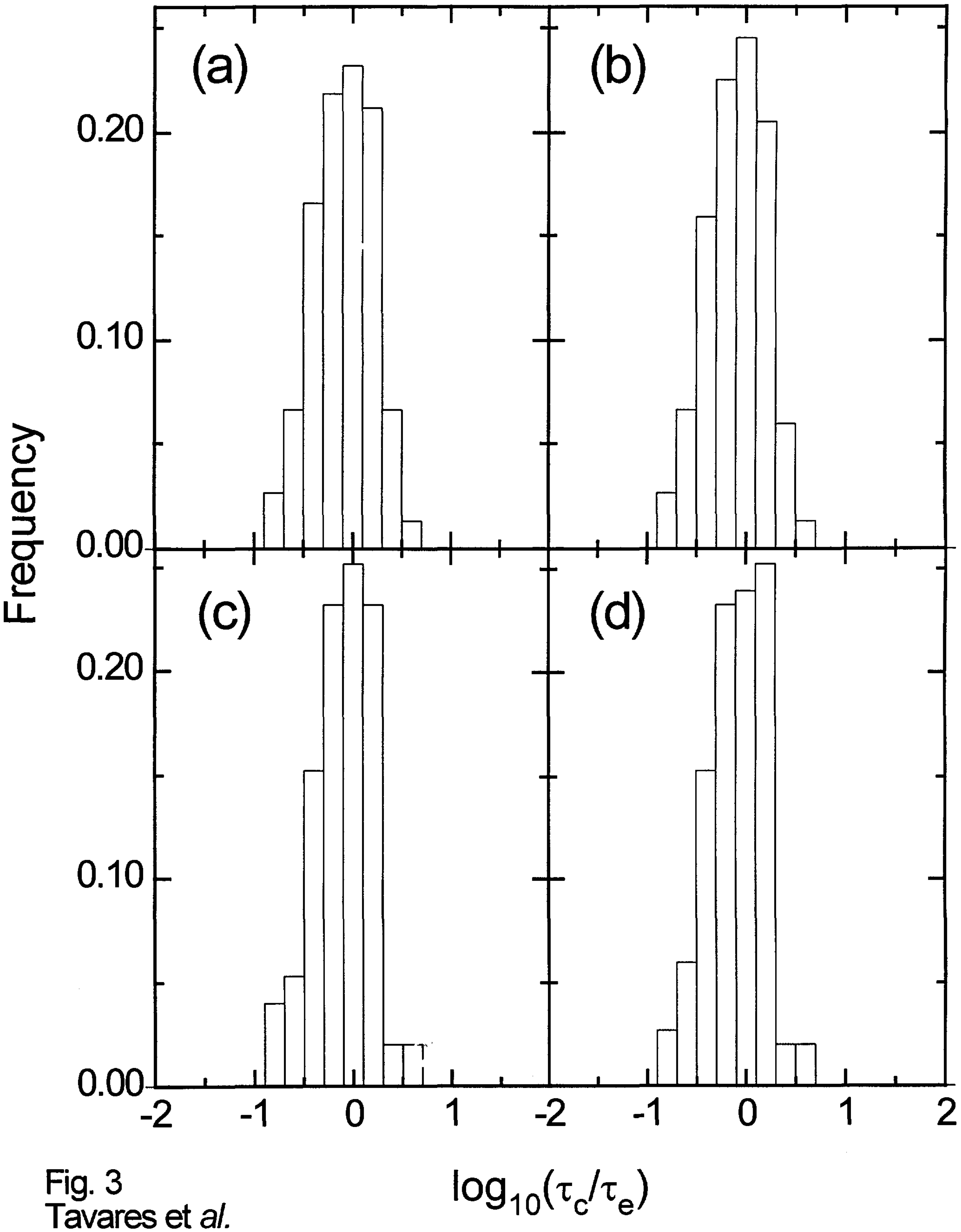

Fig. 3
Tavares et *al.*

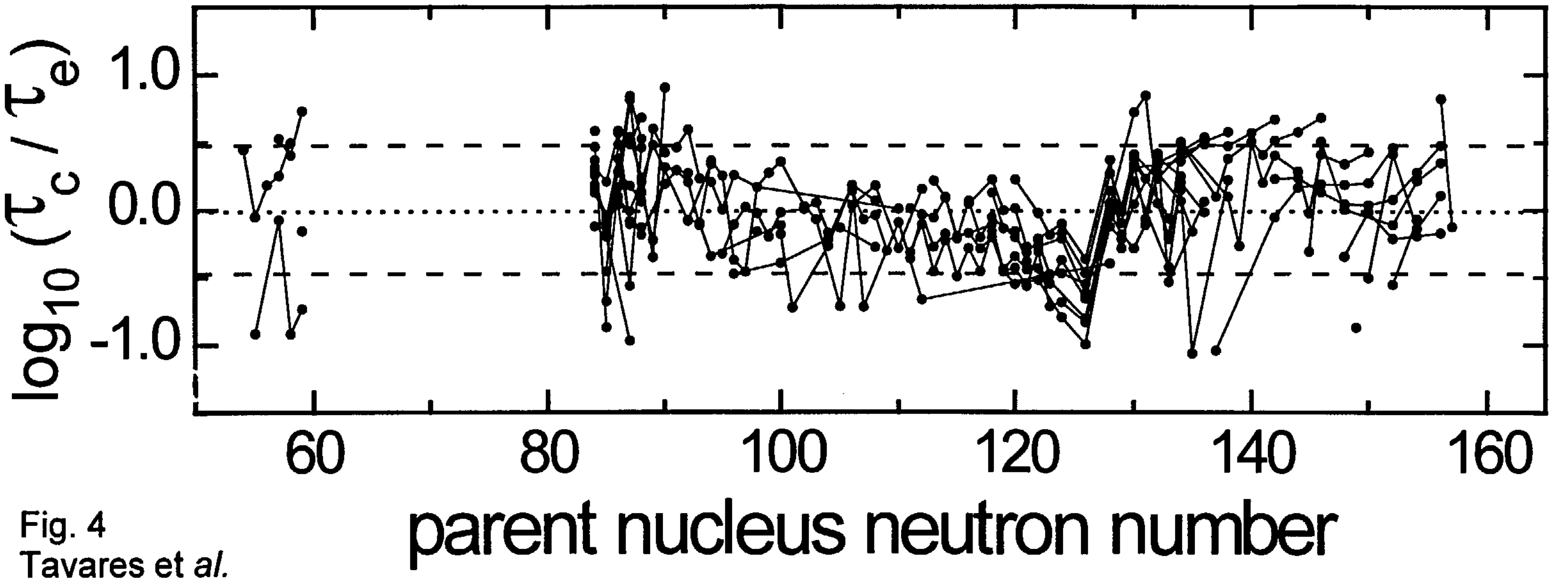

Fig. 4
Tavares et *al.*

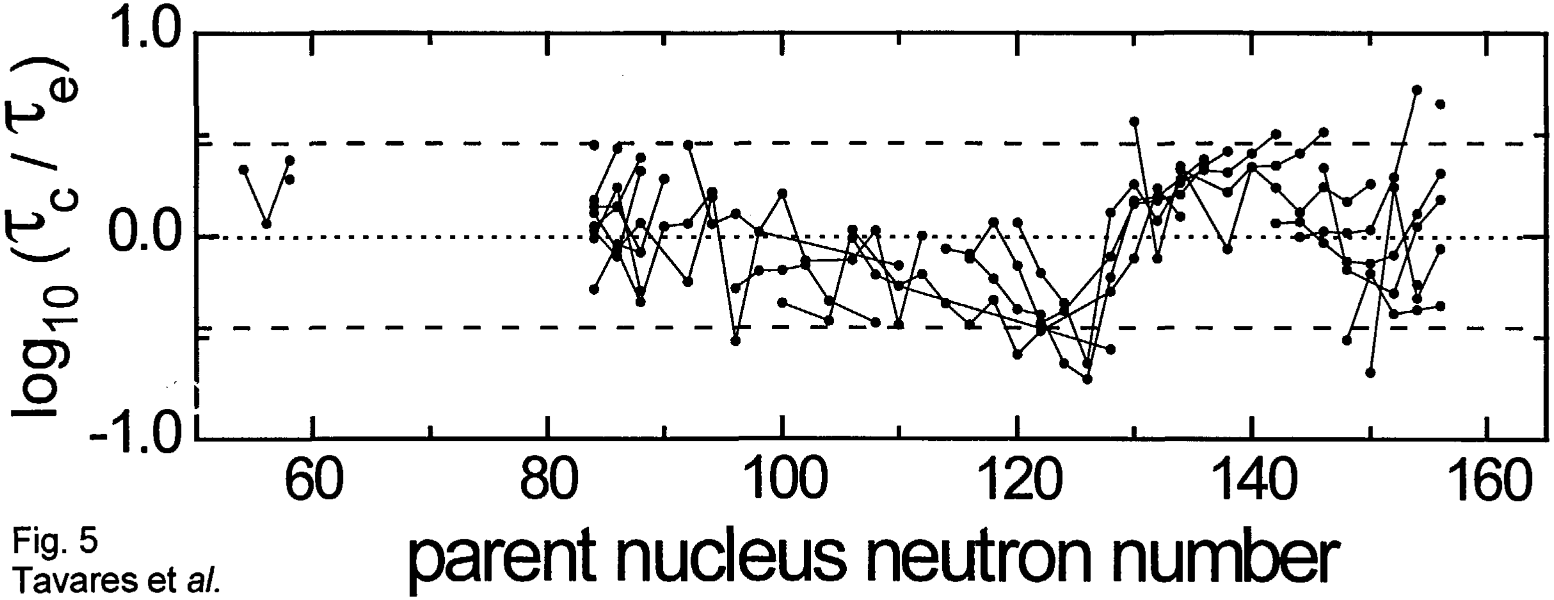

Fig. 5
Tavares et *al.*

NOTAS DE FÍSICA é uma pré-publicação de trabalho original em Física. Pedidos de cópias desta publicação devem ser enviados aos autores ou ao:

Centro Brasileiro de Pesquisas Físicas
Área de Publicações
Rua Dr. Xavier Sigaud, 150 – $4^{\underline{o}}$ andar
22290-180 – Rio de Janeiro, RJ
Brasil

NOTAS DE FÍSICA is a preprint of original unpublished works in Physics. Requests for copies of these reports should be addressed to:

Centro Brasileiro de Pesquisas Físicas
Área de Publicações
Rua Dr. Xavier Sigaud, 150 – $4^{\underline{o}}$ andar
22290-180 – Rio de Janeiro, RJ
Brazil